Applied Scientific Research 47: 221–231, 1990.

Light scattering off Brownian particles in shear flow

JOS DERKSEN & WILLEM VAN DE WATER
Physics Department, Eindhoven University of Technology, P.O. Box 513,
5600 MB Eindhoven, The Netherlands

Received 14 April 1989; accepted in revised form 30 November 1989

Abstract. Brownian motion in simple shear flow is studied using the technique of dynamical light scattering. In a conventional scattering experiment the effect of Brownian motion is obscured by that of (deterministic) particle convection. We describe an experimental setup in which both effects are separated.

1. Introduction

Light scattering has been used successfully to study solutions of Brownian particles in equilibrium. The erratically moving particle causes a fluctuating scattered light intensity, which reveals the microscopic fluctuations of the particle position. Many solutions, however, are not in equilibrium, the simplest example is a sheared solution [2, 3, 7]. At first sight, dynamic light scattering might be employed to probe the microscopic fluctuations of the particle positions in the non-equilibrium case as well. However, it turns out that in a conventional setup more mundane effects associated with shear dominate the fluctuation spectrum. Those effects, on the other hand, may be quite interesting for laser-Doppler velocimetry, because they can be exploited such as to procure the velocity gradient in a point [6]. In the present paper we discuss light scattering experiments that do provide information about the fluctuations in a fluid that undergoes shear. As the simplest possible case we will describe its application in the case of non-interacting Brownian particles.

2. Brownian motion

Colloidal particles in a host fluid exhibit Brownian motion. Collisions with thermal fluid molecules provide the stochastic driving force of this motion. The particle motion is damped by Stokes friction with the solvent fluid. The microscopic equation of motion, the Langevin equation, for a Brownian particle reads:

$$\frac{d^2\mathbf{x}}{dt^2} + \beta \frac{d\mathbf{x}}{dt} = \mathbf{F}(t), \tag{1}$$

where $\mathbf{x}(t)$ is its time-dependent position, and $\mathbf{F}(t)$ is the random force. The friction coefficient β for an isolated spherical particle with radius a, and mass m in a fluid with dynamic viscosity η is $\beta = 6\pi\eta a/m$, it is also the inverse of the characteristic time of the velocity autocorrelation function. For large times, such that $t \gg \beta^{-1}$, an equation for a probability density $P(\mathbf{x}, t)$ of the particle position may be derived from equation 1 [10]:

$$\frac{\partial P}{\partial t} = D\nabla^2 P. \tag{2}$$

The Stokes–Einstein result:

$$\langle |\Delta\mathbf{x}|^2 \rangle = 2Dt, \quad D = kT/6\pi\eta a \tag{3}$$

expresses that the mean-square displacement of a free Brownian particle is proportional to time. The diffusion coefficient D is determined by the kinetic energy of the fluid molecules, kT, and the Stokes resistance of a sphere, $6\pi\eta a$.

When a Brownian particle is subjected to simple shear ($u_x = u_0 + \gamma y$, $u_y = 0$), the Langevin equation becomes:

$$\frac{d^2x}{dt^2} + \beta \frac{dx}{dt} = \beta(\gamma y + u_0) + F_x(t),$$

$$\frac{d^2y}{dt^2} + \beta \frac{dy}{dt} = F_y(t), \tag{4}$$

where γ is the shear rate. An at first sight surprising result is that for large times, $t \gg \beta^{-1}$, the mean-square displacement of a particle is proportional to t^3 [4, 8]. Strictly speaking there is then no longer diffusive behaviour. Furthermore, the spreading of the particles becomes anisotropic; displacements in the x direction are enhanced by the flow. An intuitive understanding for this behaviour may be reached as follows. In the y direction there is ordinary diffusion with rms displacement $\Delta y \simeq t^{1/2}$. This gives rise to a displacement in the x direction of $(\Delta y\gamma)\, t \simeq t^{3/2}$, resulting in a mean-square

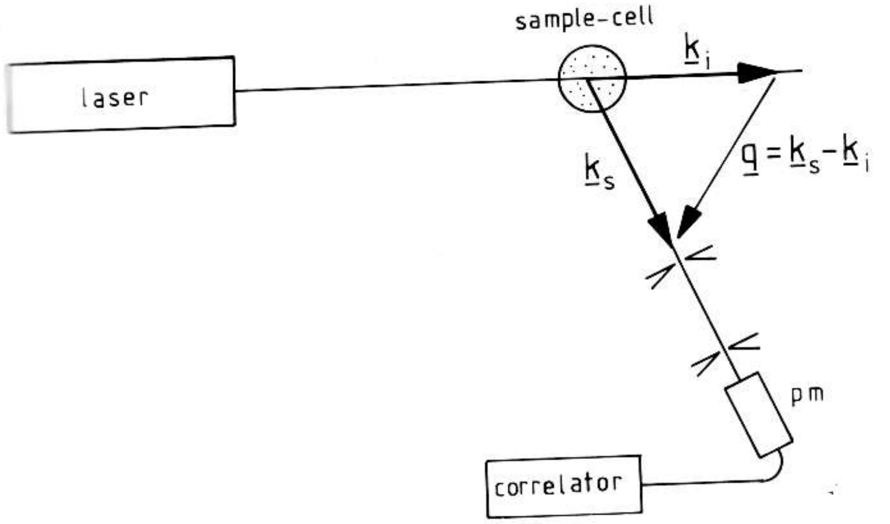

Fig. 1. Schematical experimental setup for dynamic light scattering experiments. Light with wavevector $\mathbf{k}_i$ emerges from a laser and strikes the sample cell. The scattered light wavevector $\mathbf{k}_s$ is defined through two pinholes.

displacement in x direction proportional to t^3. It is our aim to device experimental techniques that are able to reveal this anomalous diffusion on a microscopic level.

3. Dynamic light scattering

Dynamic light scattering is an excellent tool for studying Brownian motion, because motion on scales comparable to the wavelength of light can be probed. Figure 1 shows an elementary light scattering experiment. A coherent beam of light with wavevector $\mathbf{k}_i$ simultaneously hits a large number (N) of Brownian particles. The detector is arranged such as to accept light that has been scattered in the direction $\mathbf{k}_s$. At its sensitive surface the detected electric field amplitude is the sum of that scattered by particles located at $\mathbf{x}_j(t)$:

$$E(\mathbf{q}, t) = \sum_{j=1}^{N} E_0[\mathbf{x}_j(t)] e^{i\mathbf{q} \cdot \mathbf{x}_j(t)}, \tag{5}$$

where the scattering vector $\mathbf{q} = \mathbf{k}_s - \mathbf{k}_i$ and E_0 is the scattered field amplitude. The scattered electric field fluctuates in time due to the particles' Brownian motion. Information about the fluctuating particle positions is contained in the electric field autocorrelation function $G^{(1)}$:

$$G^{(1)}(\mathbf{q}, t) = \sum_{j=1}^{N} \sum_{k=1}^{N} \langle E_0^*[\mathbf{x}_k(0)] \cdot E_0[\mathbf{x}_j(t)] e^{i\mathbf{q}\cdot[\mathbf{x}_j(t) - \mathbf{x}_k(0)]} \rangle, \tag{6}$$

where the angle brackets denote an ensemble average. In the case of non-interacting Brownian particles the cross terms containing $j \neq k$ do not contribute to the sum, and equation 6 reduces to the well known result [9]:

$$G^{(1)}(\mathbf{q}, t) \simeq e^{-Dq^2 t}, \tag{7}$$

where D is the Stokes–Einstein diffusion coefficient.

A fundamental problem in the interpretation of dynamic light scattering is the relation between the desired field correlation function and the measured intensity correlation function, $G^{(2)}(\mathbf{q}, t)$. The often quoted relation:

$$G^{(2)}(\mathbf{q}, t) = 1 + |G^{(1)}(\mathbf{q}, t)|^2 \tag{8}$$

is only valid if the field fluctuations obey Gaussian statistics [9]. This is the case when the scattered light intensity is the sum of a large number of independent contributions, it is, however not the case when the particle number inside the measuring volume fluctuates significantly.

4. Dynamic light scattering in shear flow

The first study of light scattering in shear flow was reported by Fuller et al [5]. Their main interest was in point measurements of velocity gradients, no in Brownian motion. As we will demonstrate here, in a conventional exper imental setup fluctuations due to Brownian motion are obscured by modulation of the correlation function due to particles traversing the sca tering volume. To this aim we factorize the ensemble average in equation in a part involving the phases and a part involving the amplitude:

$$G^{(1)}(\mathbf{q}, t) = \sum_{j=1}^{N} I[\mathbf{x}_j(0)] \langle e^{i\mathbf{q}\cdot[\mathbf{x}_j(t) - \mathbf{x}_j(0)]} \rangle,$$

which is permitted if the linear size of the scattering volume is large wi respect to the wavelength of the used light. The particle position may written as the sum of a deterministic component due to convection an stochastic part, $\tilde{\mathbf{x}}(t)$, due to Brownian motion:

$$\mathbf{x}_j(t) - \mathbf{x}_j(0) = t(u_0 + y_j(0)\gamma)\mathbf{e}_x + \tilde{\mathbf{x}}_j(t) - \tilde{\mathbf{x}}_j(0),$$

where u_0 is the mean flow velocity in the scattering volume. Accordingly, the first-order correlation function can be written as:

$$G^{(1)}(\mathbf{q}, t) \;=\; \sum_{j=1}^{N} I(\mathbf{x}_j)\,\mathrm{e}^{\mathrm{i}q_x(u_0+y_j\gamma)t}\langle \mathrm{e}^{\mathrm{i}\mathbf{q}\cdot[\tilde{\mathbf{x}}_j(t)-\tilde{\mathbf{x}}_j(0)]}\rangle. \tag{11}$$

In case of simple shear we quote the following result for the last factor in equation 11 [5]:

$$B(\mathbf{q}, t) \equiv \langle \mathrm{e}^{\mathrm{i}\mathbf{q}\cdot[\tilde{\mathbf{x}}_j(t)-\tilde{\mathbf{x}}_j(0)]}\rangle \;=\; \mathrm{e}^{-D[q_x^2(1+(\gamma t)^2/3)-\gamma t q_x q_y+q_y^2+q_z^2]t}. \tag{12}$$

We next approximate the sum in equation 11 with an integral over the scattering volume that is defined by the cross-section of the laser beam and the acceptance cone of the light collecting optics:

$$\sum_{j=1}^{N} I[\mathbf{x}_j(0)]\mathrm{e}^{\mathrm{i}q_x(u_0+y_j\gamma)t} \;=\; \mathrm{e}^{\mathrm{i}q_x u_0 t}\int_V \mathrm{d}^3x I(\mathbf{x})\,\mathrm{e}^{\mathrm{i}q_x y\gamma t}. \tag{13}$$

The correlation function is then the product of three time-dependent factors. One is associated with Brownian motion, whereas the other two are connected with (deterministic) convection. Equation 13 embodies the convective time-scales. The time dependence contained in the first factor in the right-hand side of equation 13 will vanish when an intensity-correlation is measured and this factor will be multiplied by its complex conjugate. The second factor is a spatial Fourier transform of the intensity distribution $I(\mathbf{x})$ over the scattering volume. It is characterized by a time-scale $\tau_s = (q_x\gamma L)^{-1}$, where L is the size of the scattering volume. Generally $I(\mathbf{x})$ is a Gaussian and the second factor will decay on a time τ_s. From equation 12 it follows that the influence of shear on diffusion is observed on a time-scale $\tau_d = \gamma^{-1}$. However, this time-scale will always be much larger than τ_s: their ratio equals L/λ, that is the macroscopic size of the scattering volume over the wavelength of light. Due to the finite signal to noise ratio in the experiment only the phenomenon associated with the shortest time-scale will be observable. Thus, the influence of shear on diffusion will be obscured by the effect of the deterministic motion of the particles.

Summarizing, the naïve light scattering experiment produces a correlation function that consists of a peak at $t = 0$ whose width is inversely proportional to the size of the scattering volume. Experimental information about the diffusion factor $B(\mathbf{q}, t)$ would become accessible if one could somehow shift this peak to positive times t_0, and measure its height which is proportional to $B(\mathbf{q}, t_0)$. An inspection of equation 13 teaches that this would be

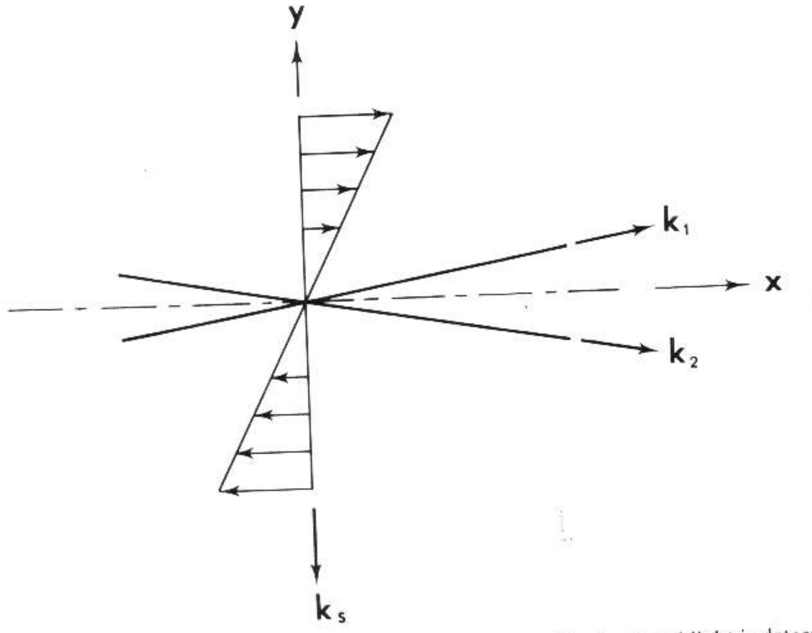

Fig. 2. Scattering geometry in shear flow with two beams $\mathbf{k}_1$, $\mathbf{k}_2$. Scattered light is detected in the direction of $\mathbf{k}_s$.

possible by adding a second scattering vector. Figure 2 shows the scattering geometry with two incident beams that has been chosen in our experiment. The electric field at the photomultiplier surface is:

$$E(\mathbf{q}_1, \mathbf{q}_2, t) = \sum_{j=1}^{N} (E_1[\mathbf{x}_j(t)]\mathrm{e}^{\mathrm{i}\mathbf{q}_1 \cdot \mathbf{x}_j(t)} + E_2[\mathbf{x}_j(t)]\mathrm{e}^{\mathrm{i}\mathbf{q}_2 \cdot \mathbf{x}_j(t)}), \tag{14}$$

where $\mathbf{q}_j = \mathbf{k}_j - \mathbf{k}_s$, $j = 1, 2$. The first-order correlation function is a sum of four terms. Two of them are the familiar $G^{(1)}(\mathbf{q}_1, t)$ and $G^{(1)}(\mathbf{q}_2, t)$, whereas the more interesting cross products read:

$$\begin{aligned} F^{(1)}(\mathbf{q}_1, \mathbf{q}_2, t) = {} & B(\mathbf{q}_2, t)\,\mathrm{e}^{\mathrm{i}q_{2x}u_0t} \int \mathrm{d}^3x E_2 E_1^* \,\mathrm{e}^{\mathrm{i}y(-\Delta q + q_{2x}\gamma t)} \\ & + B(\mathbf{q}_1, t)\,\mathrm{e}^{\mathrm{i}q_{1x}u_0t} \int \mathrm{d}^3x E_2^* E_1 \,\mathrm{e}^{\mathrm{i}y(\Delta q + q_{1x}\gamma t)}, \end{aligned} \tag{15}$$

where $\Delta\mathbf{q} = \mathbf{q}_1 - \mathbf{q}_2$ is chosen perpendicular to the flow direction: $\Delta\mathbf{q} \cdot \mathbf{x} = \Delta q y$. The two Fourier integrals over the mixed profile functions $E_2E_1^*$ and $E_2^*E_1$ in equation 15 are similar to that in equation 13, however, the origin of time is shifted to $t_0 = \Delta q/(q_{2x}\gamma)$, and $t_0 = -\Delta q/(q_{1x}\gamma)$, respectively.

Provided that the physics of the present experiment allows application of the Siegert relation (equation 8), the intensity correlation function equals one plus the square of $|G^{(1)}(\mathbf{q}_1, t) + G^{(1)}(\mathbf{q}_2, t) + F^{(1)}(\mathbf{q}_1, \mathbf{q}_2, t)|$. The resulting correlation function will therefore have two peaks, one is located at $t = 0$ and is described by $|G^{(1)}(\mathbf{q}_1, t) + G^{(1)}(\mathbf{q}_2, t)|^2$, the other one is located at $t = \Delta q/(q_{2x}\gamma)$. Because the peaks are shifted in time with respect to one another, squaring leads to vanishing cross products. The secondary peak results from the first term on the right-hand side in equation 15, the height of this peak is gauged by $|B(\mathbf{q}, t)|^2$. The phase factor in equation 15, involving u_0 will give rise to a unity prefactor in case of intensity correlation. The position t_0 of the secondary peak can be varied by varying $\Delta\mathbf{q}$, i.e. by varying the mutual beam angle, or by changing the shear rate γ.

5. Experimental

The scattering geometry of Fig. 2 was realised in the experimental setup shown in Fig. 3. The flow was generated in a Couette device with

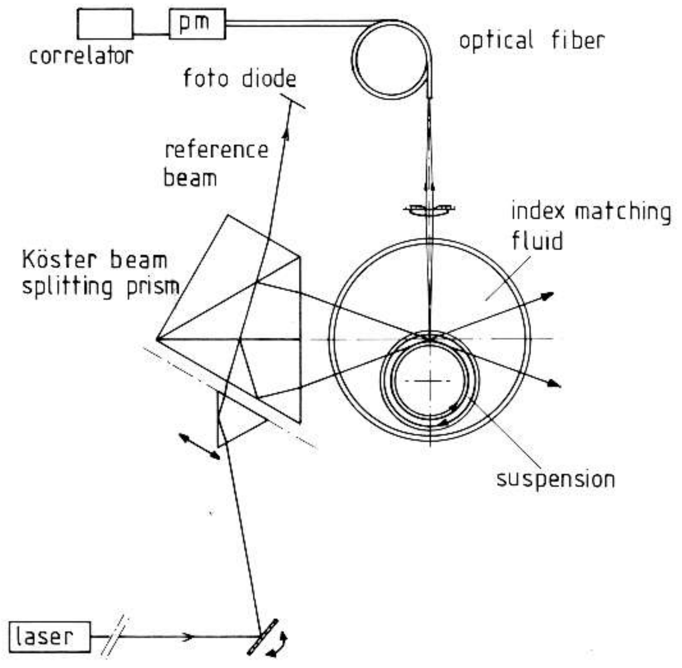

Fig. 3. Experimental setup described in this article. Two laser beams cross between the counter-rotating cylinders of a Couette device, the reference beam is used to monitor the position of the scattering volume.

counter-rotating cylinders. The radial position of the center of the scattering volume was chosen such that $u_0 = 0$, this ensured that number fluctuations due to flow will be small. In order to facilitate the adjustment of the location of the scattering volume, a glass cylinder is placed concentric with the scattering volume. All of the apparatus within its perimeter, including fluid and glass cylinders of the Couette apparatus, had a uniform refractive index at $\lambda = 514.5$ nm. The index matching fluid in which the particles were suspended was a mixture of tetraethylene glycol and glycerol. We used polystyrene spheres with 0.19 μm diameter and volume fraction 2.5×10^{-5}. The laser beam emerged from an Argon ion laser operated at 514.5 nm, and was subsequently divided into three parts in a modified Köster prism. Two beams entered the Couette device, the third beam was used to check and control the position of the crossing region in the fluid. This setup enabled us to alter the beam crossing angle while keeping the crossing region fixed in space by rotating a mirror and translating a small prism such that the reference beam remained at a fixed position. A quadrant diode monitored the reference beam position to an accuracy of approximately 5 μm. Scattered

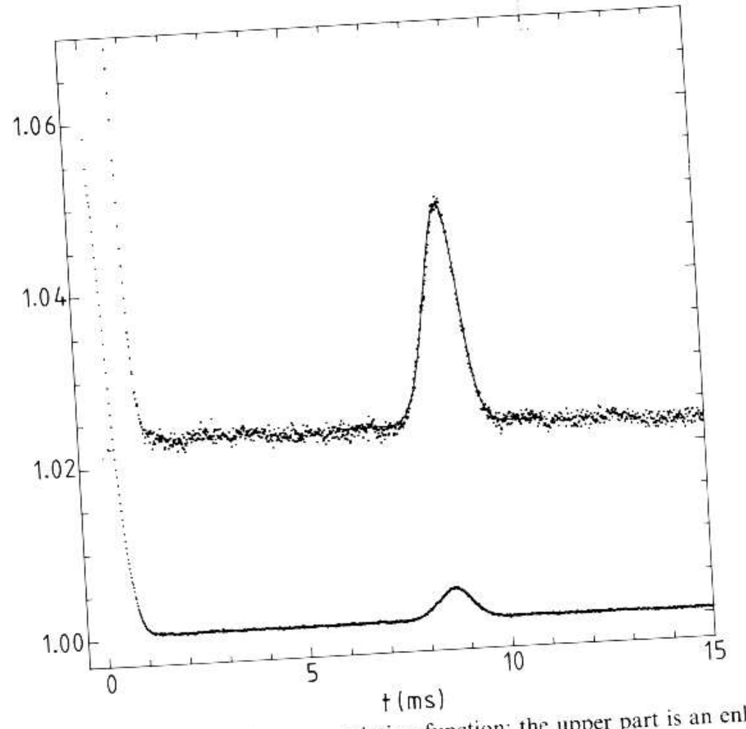

Fig. 4. Measured normalized photon correlation function; the upper part is an enlargement of the lower part. The full line represents a Gaussian function that has been fitted to the experimental results.

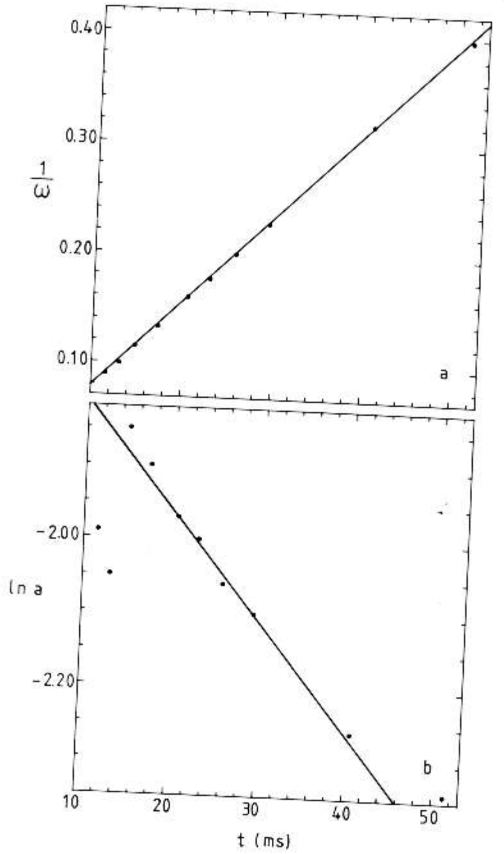

Fig. 5. (a) Dots: position of the secondary peak as a function of inverse angular velocity. Full line: expected behaviour for a mutual beam angle of 16°. (b) Dots: log of height of secondary peak as a function of delay time. Full line: prediction based on equation 12 (see text), the line has been shifted vertically.

light passed through a pinhole–lens combination and was transported to the photomultiplier using a multimode optical fiber. The photomultiplier signal consists of a time series of pulses, each pulse representing a detected photon. After amplification and discrimination the logical photon signal was fed into a digital correlator. The measured photon correlation function is proportional to the intensity, or second-order, correlation function.

A proper definition of the scattering volume in this experiment requires that three lines pass through one point, namely the two incident beams and the line defined by the collecting optics. The analysis sketched in the previous section implies that misalignment of the detector optics results in oscillatory correlation functions. This observation was used as a tool for alignment: the detector was adjusted by micrometer screws such that the correlation function ceased to show oscillations. The size of the resulting scattering volume was $30 \times 100 \times 100\,\mu$m.

6. Results and conclusions

Figure 4 shows an example of a measured double-peaked photon correlation function. The two relevant parameters, the position and the height of the secondary peak are found by fitting a Gaussian function. Figure 5a shows the secondary peak position as a function of the inverse rotating velocity $\omega(\simeq \gamma^{-1})$ of the counter-rotating cylinders of the Couette device. The two incident beams cross under an angle of 16°. The predicted relation between t_0 and γ is also drawn in the figure, and demonstrates that the present setup allows point measurements of shear rates. Figure 5b shows the log of the measured secondary peak height as a function of the peak delay time t_0. The delay time was varied by varying the shear rate while keeping the beam crossing angle constant, as a consequence, the product $\gamma t (= \Delta q / q_x)$ is also constant. At a beam crossing angle of 16° and a scattering wavevector $\mathbf{k}_s$ which is perpendicular to the bisector of the incident beams, $\gamma t = 0.28$. When γt is constant, $B(\mathbf{q}, t)$, which embodies the Brownian motion, is a negative exponential function of time (equation 12). This is in agreement with the observed behavior, however, deviations are evident at short times (high shear rates), and long times (low shear rates). Work is in progress to elucidate their cause.

There have been earlier reports of an attempt to measure Brownian motion in a sheared fluid [1]. The present experiment is, to our knowledge, the first to demonstrate the feasibility of a two-beam setup. Apart from the fundamental interest in obtaining information about non-equilibrium fluids, there are a few important practical ramifications. First, we have again demonstrated the possibility of point measurements of the shear rate [6]. Second, our method could be used to obtain information about the sizes of particles in a sheared fluid; this would be of relevance in those situations where the particle size may alter due to shear stress. There are also quite a few experimental intricacies which still need to be mastered. The most important experimental circumstance is the definition of the scattering volume, which requires an extremely stable setup.

References

1. Ackerson, B.J. and Clark, N.A.: Dynamic light scattering at low rates of shear. *Journal de Physique* 42 (1981) 929–936.
2. Beyens, D., Gbadamassi, M. and Boyer, L.: Light-scattering study of a critical mixture with shear flow. *Physical Review Letters* 43 (1979) 1253–1256.

3. Clark, N.A. and Ackerson, B.J.: Observation of the coupling of concentration fluctuations to steady-shear flow. *Physical Review Letters* 44 (1980) 1368–1371.
4. Foister, R.T. and van de Ven, T.G.M.: Diffusion of Brownian particles in shear flow. *Journal of Fluid Mechanics* 96 (1980) 105–132.
5. Fuller, G.G., Rallison, J.M., Schmidt, R.L. and Leal, L.G.: The measurement of velocity gradients in laminar flow by homodyne light-scattering spectroscopy. *Journal of Fluid Mechanics* 100 (1980) 555–575.
6. Keveloh, C. and Staude W.: Determination of velocity gradients with scattered light cross-correlation measurements. *Applied Optics* 22 (1983) 333–338.
7. Machta, J., Oppenheim, I. and Procaccia, I.: Light scattering and pair-correlation functions in fluids with nonuniform velocity fields. *Physical Review Letters* 42 (1979) 1368–1371.
8. San Miguel, M. and Sancho, J.M.: Brownian motion in shear flow. *Physica* 99A (1979) 357–364.
9. Schaetzel, K.: Correlation techniques in dynamic light scattering. *Applied Physics* B42 (1987) 193–213.
10. Wang, M.C. and Uhlenbeck, G.E.: On the theory of Brownian motion. *Review of Modern Physics* 17 (1945) 323–342.